AIAA 80-1284R

Critical Considerations in the Design of Supersonic Combustion Ramjet (Scramjet) Engines

P.J. Waltrup,* F.S. Billig,† and M.C. Evans‡
The Johns Hopkins University Applied Physics Laboratory, Laurel, Md.

The design and estimation of the performance of a supersonic combustion ramjet (scramjet) engine is critically dependent on the geometry and efficiency of each of the engine components. Therefore, it is mandatory to be cognizant of all the available experimental data and theoretical modeling that has been established if a credible design is to be obtained. The purpose of this paper is to reiterate norms for component geometries, lengths, internal losses, and combustion kinetics that have been established and/or substantiated in the technical literature and to illustrate the sensitivity of engine performance to deviations from those norms. A specific exemplary engine design is presented and used to illustrate these effects. The results show that the maximum predicted net engine thrust can be overestimated by as much as 45% if more idealistic assumptions, similar to those used in the design of conventional subsonic combustion ramjet engines, are used.

Nomenclature

A = area
$\bar{C}_f$ = average skin friction coefficient
C_{D_a} = vehicle axial drag coefficient based on A_i
$C_{D_{\text{add},1e,I}}$ = inlet additive, leading engine, and total drag coefficients, respectively, based on A_i
$C_{T_{g,n}}$ = gross and net engine internal thrust coefficient, $C_{T_n} = C_{T_g} - C_{D_I}$, based on A_i
ER = fuel-air equivalence ratio
f = fuel-air ratio
f_s = stoichiometric fuel-air ratio
F = stream thrust
h_f = fuel enthalpy
Δh = enthalpy difference used in Fig. 5, defined in Ref. 1
ΔH_f = fuel lower heating value
L = length
M = Mach number
n_A = axial acceleration (g's)
P = pressure
$\bar{Q}$ = average total heat flux
T = temperature, thrust
u = velocity
$\dot{w}$ = flow rate
Z = altitude
γ = ratio of specific heats
$\bar{\tau}$ = average shear stress
θ = boundary-layer momentum thickness
ρ = density
η_c = fuel combustion efficiency
η_{KE} = inlet kinetic energy efficiency
η_n = nozzle efficiency

Subscripts

0-5 = axial stations given in Fig. 1
c = combustor
d = air duct
f = fuel
i = inlet
n = nozzle
o = free stream
t = stagnation condition
w = wall

Superscript

$\bar{(\ )}$ = average value

Presented as Paper 80-1284 at the AIAA/SAE/ASME 16th Joint Propulsion Conference, Hartford, Conn., June 30-July 2, 1980; submitted Oct. 20, 1980; revision received Feb. 19, 1981.

*Section Supervisor, Supersonic Combustion, Propulsion Group. Associate Fellow. AIAA.
†Assistant Division Supervisor, Aeronautics Division. Fellow AIAA.
‡Engineering Assistant, Propulsion Group. Associate Member AIAA.

Introduction

THE design of efficient hypersonic ramjet engines, where the primary mode of combustion occurs in a supersonic rather than a subsonic air stream, requires special consideration in a number of areas not normally considered in the design of more-conventional subsonic combustion ramjets. Specifically, if a supersonic combustion ramjet (scramjet) engine is to fly over a reasonable Mach-number range, e.g., $M_0 = 4\text{-}7$, the area-contraction ratio of the inlet diffuser and the area ratio and area distribution of the combustor must be selected to meet the low Mach number performance requirements yet permit good engine performance at the high Mach number cruise condition. Since the two flight conditions require different inlet and combustor area ratios, a compromise must be reached. Strong interactions between the inlet and combustor require that consideration be given to the design of an isolator air duct to prevent the compression waves generated by the supersonic combustion process at the entrance of the supersonic combustor from interacting with the inlet diffuser's flowfield. Furthermore, because of the short residence times available in a supersonic combustor, a highly reactive fuel, such as a borane or an aluminum alkyl, or a more conventional heavy hydrocarbon fuel, such as a JP or RJ, with a very reactive pilot or additive fuel is required if a reasonable fuel combustion efficiency is to be maintained, especially at the lower M_0. Although equilibrium thermochemistry is not, in general, present in the combustor, combustor performance can be predicted assuming equilibrium thermochemistry by including nonequilibrium effects in the fuel combustion efficiency. Wall skin friction and total pressure losses in the isolator, combustor, and exit nozzle are also important because their absolute values are significant when compared to the overall engine total pressure losses. In addition, the flow entering the exit nozzle is generally nonuniform and does not pass through a throat, thereby complicating the design of the exit nozzle contour and generally preventing the minimization of divergence losses. Finally, because of the high Mach numbers and temperatures associated with scramjet operation, equilibrium ther-

mochemistry cannot, in general, be assumed in the nozzle expansion process. Consequently, the presence of some frozen species in the expansion reduces overall engine thrust from the level that would result from an equilibrium expansion.

In Ref. 1, an analytical model based on an integral approach was presented for predicting scramjet engine performance. Included in this paper was the methodology required for selecting the optimum inlet area contraction ratio, combustor area ratio, and exit nozzle expansion ratio in accordance with prescribed engine design constraints and flight conditions. The results presented and assumptions used in Ref. 1 were based on experimental data and analytical techniques developed from testing and analyzing scramjet engines and components over the past 20 yr (see Ref. 2). The engine configuration used in Ref. 1 was conventional nose entry. The methodology, however, is not limited to this configuration. Consequently, in this paper, a configuration that typifies the so-called "airframe integrated" scramjet[2,3] will be examined, and the analysis will be extended to show the sensitivity of the overall engine performance to inlet total pressure recovery (kinetic energy efficiency), isolator air duct and combustor length, fuel type, wall skin friction, nozzle efficiency, and engine thermochemistry which were not discussed in Ref. 1. Since overall scramjet engine performance is quite sensitive to deviations from the established norms in each of these areas, the basis for establishing these norms and the sensitivity of engine performance to deviations therefrom will be discussed. The order of presentation will be to first design an optimum engine geometry using the established component norms and then to illustrate and discuss the sensitivity of this engine design to variations in inlet kinetic energy efficiency, air duct and combustor length, wall skin friction, fuel type, nozzle efficiency, and thermochemistry.

Optimized Fixed-Geometry Scramjet-Engine Design

Design Requirements and Constraints

Since engine optimization is dependent on the mission of the vehicle under consideration, a specific mission is specified for this example. In particular, the vehicle is assumed to be a two-stage rocket-boosted missile propelled by a fixed-geometry scramjet engine during the sustain portion of flight. It is to have a high accelerative capability from its end-of-rocket-boost $M_0 = 4$ condition to its cruise condition at $M_0 = 7$ and have high lateral maneuverability. For simplicity, it is assumed that the entire sustain portion of flight occurs at an altitude of 50,000 ft (15.24 km). The principal consideration in selection of the engine is assumed to be a high-thrust capability. Thrust efficiency, i.e., thrust per unit fuel-flow rate, is also an important parameter in configuration selection, especially if range is an important element in the mission requirements, but is considered secondary herein. Although most missiles must also fit within a prescribed packaging volume, no such constraint has been imposed here in order to permit selection of the optimum exit nozzle expansion ratio for the scramjet engine.

For simplicity, and to be consistent with some of the engine configurations that have been proposed, such as those in Refs. 2 and 3, it is assumed that the scramjet inlet is located beneath the main body (Fig. 1a) and sufficiently far aft that the effects of forebody compression are negligible. It is also assumed that the exit nozzle of the engine is an integral part of the missile afterbody. By so doing, the problem of analyzing the complex engine airframe interaction that would be present in the truncated nozzle configuration often shown for "airframe integrated" scramjet[3] is eliminated. Moreover, this results in the largest possible net force coefficient because base drag is eliminated and the increased engine thrust due to the confined nozzle expansion more than compensates for the additional nozzle friction losses. Although the engine need not be two-dimensional, most of the available experimental data on piloted, liquid-fueled scramjet engines in the open literature[2,4,5] is for this configuration. Consequently, a two-dimensional engine has been assumed herein.

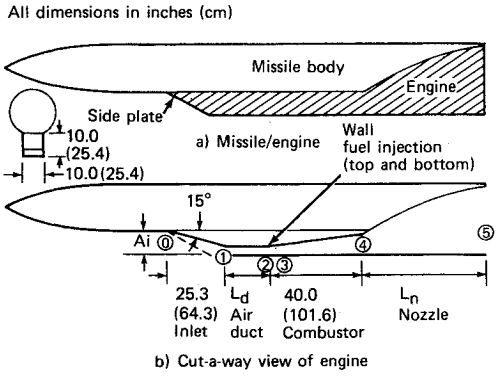

Fig. 1 Schematic of scramjet engine and missile configuration.

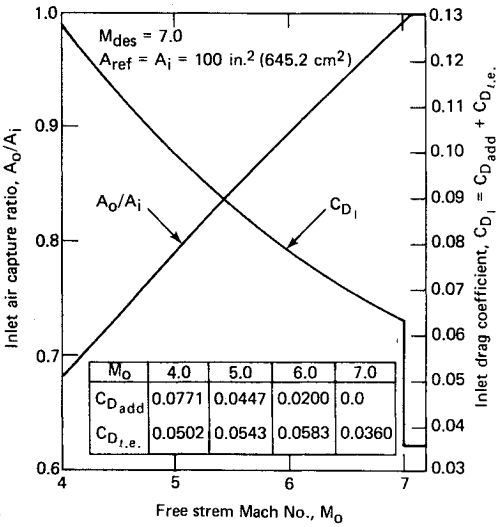

Fig. 2 Inlet air capute and drag characteristics, $M_{DES} = 7.0$.

Configuration Selection

Given the previous constraints and objectives, the first phase of the optimum engine design study is to select an appropriate inlet design, air duct and combustor length, fuel type, and nozzle efficiency and length using experimentally verified norms where possible. Then the optimization procedure presented in Ref. 1 will be used to select the values of inlet area contraction ratio A_i/A_1, combustor exit to inlet area ratio A_4/A_2, and nozzle exit to diffuser inlet area ratio A_5/A_i, which will yield the highest average net engine thrust coefficient $C_{T_{n,\max}}$ over the specified flight regime of $M_0 = 4$ to $M_0 = 7$ at 50,000 ft (15.24 km). Here C_{T_n} is defined as the gross internal engine thrust coefficient C_{T_g} minus the inlet drag coefficient C_{D_I} consisting of additive $C_{D_{add}}$ plus leading edge $C_{D_{le}}$ drag. In all cases, the reference area is taken to be A_i.

To readily obtain estimates for the air capture and $C_{D_{add}}$, a simple inlet geometry has been assumed. The compression ramp consists of a 15 deg wedge followed by a curved surface that produces compression waves that are reflected from the flat inner cowl surface. The wedge shock strikes the cowl lip at $M_0 = M_{DES} = 7$, i.e., full capture is reached at $M_0 = 7$. The first compression wave from the curved surface strikes the cowl lip at $M_0 = 4$; therefore at $M_0 > 4$ all of the compression waves other than the wedge shock fall downstream of the cowl lip. Additional details of the compression process, such as starting, have not been considered. Instead, it is assumed that the flow is one-dimensional at station 1 with properties consistent with the values of η_{KE} cited below and with no side spillover. For this study the inlet is a 10×10 in.^{2} (25.4×25.4 cm^2) square as illustrated in Fig. 1b so $A_i = 100$ in.^{2} (545.2 cm^2). The engine's internal width is a constant 10 in. (25.4 cm). Figure 1b also shows the numbered engine stations (0-5) used throughout the remainder of this study. Forebody-

precompression effects on the inlet air capture ratio A_0/A_i and kinetic energy efficiency η_{KE} has been assumed negligible and all calculations are for 0 deg angle-of-attack. A leading-edge diameter of 0.1 in. (0.25 cm) has been assumed for the side plates and cowl lip. With these assumptions, A_0/A_i and the inlet drag coefficients were calculated and are given in Fig. 2 as a function of M_0. Here, A_0/A_i varies between 0.6798 and 1.00 and C_{D_I} varies between 0.1276 and 0.036 at $M_0=4$ and 7, respectively. Based on previous hypersonic air inlet designs,[1,2] η_{KE} was assumed to vary linearly between 0.98 at $M_0=4$ and 0.95 at $M_0=8$ regardless of the inlet's geometric area contraction ratio A_i/A_1. Note that η_{KE} would be expected to decrease slightly with increasing A_i/A_1, but for simplicity, this effect was ignored. A lower M_{DES} would affect η_{KE} and for $M_0<M_{DES}$, increase A_0/A_i and lower C_{D_I}. However, varying M_{DES} would not enhance the comparisons made in the last section of this paper and might unnecessarily complicate or confuse the results presented.

With the inlet characteristics established, the next step is to select the minimum length of air duct L_d (Fig. 1b) needed to prevent the precombustion shock/boundary-layer interaction region present at the entrance of the supersonic combustor (station 2, Fig. 1b) from causing interference with the inlet flowfield. If provisions are not made to isolate the combustor and inlet, the resulting interaction can decrease A_0/A_i and increase $C_{D_{add}}$ (Ref. 6) at a given M_0, resulting in significant reduction in C_{T_n} and even reverse flow. For simplicity, the isolator duct in this study is assumed to have a constant area, i.e., $A_1=A_2$. The procedure used to determine its length is based on the semiempirical analysis developed in Refs. 6-8 assuming a duct skin friction coefficient $C_{fd}=0.00181$ and a boundary-layer momentum thickness at station 2 in the absence of a precombustion shock wave θ_2 of 0.015 in. (3.8 cm), based on the experimental results of Refs. 7 and 9. Air with a chemical composition of 0.2095 O_2, 0.7809 N_2, and 0.0096 A by volume in chemical equilibrium was assumed in all cases based on the thermochemical properties of Ref. 10 and the computational procedure of Ref. 11.

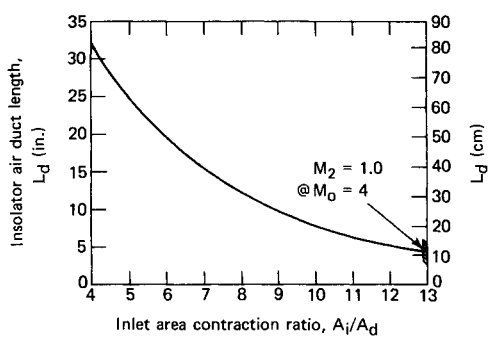

Fig. 3 Required isolator air duct length as a function of inlet area contraction ratio.

Figure 3 presents the resulting values of L_d as a function of A_i/A_1. Here, the required value of L_d decreases monotonically from 32.1 in. (81.5 cm) for $A_i/A_1=4$ to 5.2 in. (13.2 cm) for $A_i/A_1=12$. This trend of decreasing L_d with increasing A_i/A_1 is due to the decreasing effective duct diameter for a fixed A_i and decreasing M_2 (Ref. 7). Although this trend reduces the overall engine length, weight, and air duct wall skin friction losses, it also lowers M_2 which, in turn, may limit the maximum amount of heat that can be added in the combustor to less than stoichiometry for high values of A_i/A_1, especially at the lower M_0. This "combustor thermal-choking limit" will be clarified and discussed in subsequent discussions in this paper. Note also that values of $A_i/A_1>12.85$ are not possible in this fixed-geometry engine since the exit of the air duct would be choked ($M_2=1$) at $M_0=4$ when $A_i/A_1=12.85$. Since the throat of a scramjet inlet must be sized to maintain M_2 high enough to permit sufficient heat to be added to produce a reasonable net thrust coefficient at the lower M_0, an upper limit on A_i/A_1 of 12 has been assumed for the remainder of this study.

The combustor length L_c chosen for these studies is 40 in. (101.6 cm), which is approximately the same length as that used in the two-dimensional scramjet combustor and engine experiments reported in Refs. 4 and 5. Normal wall fuel injection between station 2 and 3 (Fig. 1b) is assumed in all cases. The fuel assumed in these studies closely corresponds to that used in Refs. 4 and 5, i.e., a heavy hydrocarbon piloted with chlorine trifluoride (ClF_3). In this study, however, Shelldyne-H (RJ-5, $C_{14}H_{18}$) was substituted for JP-7. Shorter combustor lengths, 20-30 in. (50.8-76.2 cm), are possible if more reactive fuels or fuel blends (such as boranes or borane/heavy hydrocarbon mixtures) are used.[2] However, very little experimental data is available in the open literature on scramjet engines using these fuels.[2,12,13].

Table 1 lists the properties of RJ-5 and ClF_3 as well as the weight percent of ClF_3 needed to ensure good combustion of the fuel-air mixture in the prescribed L_c as a function of air total temperature T_{t_0} (or M_0 and altitude). Also included are the lower heating values ΔH_f of various weight-percent mixtures of RJ-5/ClF_3 and the 21 principle products of combustion.[10,11] The weight percents of ClF_3 as a function of T_{t_0} (or M_0) are based on the data presented in Refs. 4 and 5.

Table 1 Fuel/pilot mixture properties

Basic fuel and oxidizing pilot properties

Name	Chemical formula	h_f (Btu/lbm)	ΔH_f (Btu/lbm)	Mol. Wt.	f_s
Shelldyne-H (RJ-5)	$C_{14}H_{18}$	193.24	17942	186.30	0.07284
Chlorine trifloriude	ClF_3	−719.73	–	92.46	–

Required fuel/pilot mixtures and properties

M_0	T_{t0}[a] (°R)	ClF_3[a] Wt. %	$C_{14}H_{18}$[b] Wt. %	h_f (Btu/lbm)	ΔH_f (Btu/lbm)	Mol Wt.	f_s
4.0	1593	25	75	−35.02	15591	162.84	0.10077
5.0	2214	15	85	56.29	16603	172.22	0.08737
6.0	2931	10	90	101.94	17070	176.91	0.08192
7.0	3723	10	90	101.94	17070	176.91	0.08192

Principle products of mixture equilibrium combustion[c] with air[d]

A, C, CO_2, Cl, Cl_2, ClH, ClHO, ClO, F, FH, H, HO, H_2, H_2O, N, N_2, NO, NO_2, O, O_2

[a] Total temperature at 50,000-ft (15.24-km) altitude.
[b] Based on experimental data in Refs. 4 and 5.
[c] Based on Refs. 10 and 11.
[d] Air: 0.023145 O_2, 0.7553O N_2, 0.01325 A by weight.

The required amounts of oxidizer are 25% ClF_3 at $T_{t_0}=1593°R$ (885 K) ($M_0=4$), 15% ClF_3 at $T_{t_0}=2214°R$ (1230 K) ($M_0=5$), and 10% ClF_3 for $T_{t_0}\geq 2931°R$ (1628 K) ($M_0\geq 6$) when flying at 50,000 ft (15.24 km) altitude. From Table 1, it is apparent that the necessity of using an oxidizing pilot (ClF_3) to obtain reasonable combustion efficiency ($\eta_c>80\%$) reduces the amount of heat release available for the engine. For example, at $M_0=4$, ΔH_f is 13.1% lower for the 25%/75% mixture than for pure RJ-5. Consequently, it is essential that the proper mixture be used when predicting engine preformance. Otherwise, engine performance estimates and vehicle range will be incorrect. The magnitude of these differences will be discussed later in this paper.

In addition to establishing the required combustor length and fuel composition, a reasonable range of combustor exit-to-inlet area ratios A_4/A_2 and reasonable representations of the average combustor wall skin friction coefficient $\bar{C}_f$ and heat transfer $\bar{Q}_w$ are needed to optimize the design of this engine. In order to bracket the optimum A_4/A_2 that will be determined in the next section, values between 1 and 5 were assumed for this study. Their corresponding internal wetted-wall areas A_w were then computed as a function of A_i/A_1 and A_4/A_2 for $L_c=40$ in. (101.6 cm). In each case, area divergence was obtained by assuming a constant width combustor with a flat bottom wall and a linearly diverging upper wall as shown in Fig. 1b. No geometric corrections were made to account for the boundary layer.

The skin friction and heat transfer coefficients for these types of flows can be obtained either by rigorous solutions of the boundary-layer equations[14,15] or from data correlations. The latter was chosen herein. Figure 4 shows the heat flux and shear parameters that have been adopted. They are based on correlations of experimental data from a variety of fuels and combustor geometries over a wide range of initial conditions.[2,14] The average heat transfer rate per unit surface area, $\bar{Q}_w/A_w$, is normalized by the inlet mass flux, $\dot{w}_2/A_2$, and the average gas-wall enthalpy difference Δh defined in Refs. 1 and 14. A modified Reynolds analogy is used to relate $\bar{Q}_w$ to $\bar{C}_f$, where $\bar{C}_f=2\bar{\tau}_w/\rho_2 u_2$. Here, $\bar{\tau}_w$ is the average shear stress acting on the combustor wall, and u_2 is used as the average velocity since the deceleration effects due to the precombustion shock and heat addition are about cancelled by the accelerating effects due to combustor divergence.[14] For additional details, the reader is referred to Refs. 1 and 14. From Fig. 4, it is apparent that the value of $\bar{C}_f$ increases dramatically with increasing heat release or fuel-air equivalence ratio ER. In fact, for ER = 1.0 the value of $\bar{C}_f$ is approximately 2.7 times the no-heat release value. This experimentally deduced trend of increasing $\bar{C}_f$ with ER has also been predicted in recent axisymmetric supersonic mixing and combustion analyses.[16] Consequently, combustor total pressure losses due to wall skin friction can be quite high and must be accurately modelled and accounted for if accurate predictions of engine performance are to be made. The extent of this effect will be examined in the exemplary cases presented at the end of this paper.

The final four variables needed to begin the engine optimization are nozzle exit-to-inlet area ratio A_5/A_i, length L_n, efficiency η_n, and thermochemistry. Since determining A_5/A_i is part of the optimization procedure in the next section, it is sufficient to state here that values between 1.0 and 4.0 were assumed for this study. L_n and η_n were determined using the analytical procedures presented in Ref. 17 and verified in the free-jet engine tests discussed in Ref. 2. Since the optimum L_n is a function of A_5/A_4 and the properties at station 4, its value will be determined as part of the optimization procedure in the next section. However, in all cases, the maximum average value of η_n in a fixed-geometry nozzle is about 0.975 which includes wall friction, nonuniformity, and divergence losses.

The thrust of a scramjet engine can be expressed as

$$T=\eta_n F_5-[F_0+P_0(A_5-A_0)] \qquad (1)$$

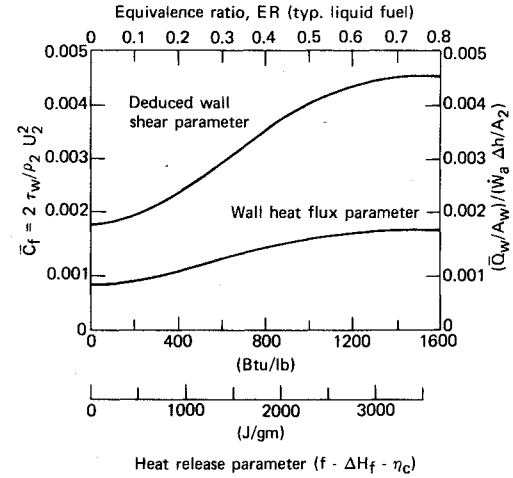

Fig. 4 Combustor wall heat transfer and skin friction coefficient as a function of fuel-air equivalence ratio.

with both the nozzle exit stream thrust F_5 and the bracketed term being large numbers. Therefore, small changes in either η_n or F_5 can have a significant effect on the predicted engine thrust and care must be taken in using the proper realistic values. The value of F_5 is dependent on the thermochemistry in the nozzle. Previous experience in both connected-pipe combustor and free-jet engine tests[2,17] have shown that the nozzle expansion process is not in thermodynamic equilibrium and that the flow properties in the nozzle exit more nearly correspond to an expansion that is chemically frozen near the nozzle entrance. The best correlation was obtained by assuming the flow to be in chemical equilibrium at the nozzle entrance, calculating F_5 (frozen) and F_5 (equilibrium) and letting $F_5=\frac{2}{3}F_5$ (frozen) + $\frac{1}{3}F_5$ (equilibrium).

Engine-Optimization Procedure

With the individual component lengths, geometries, and efficiencies as well as wall skin friction and heat transfer and engine thermochemistry established, a complete engine performance map was generated where in M_0, A_i/A_1, A_4/A_2, and A_5/A_i were varied over the previously specified range of values of each. In each case, the integral engine cycle analysis presented in Ref. 1 was used assuming standard atmospheric conditions at 50,000-ft (15.24-km) altitude,[18] equilibrium thermochemistry from stations 0 to 4, and equilibrium and frozen thermochemistry in the nozzle. In addition, wall heat losses were assumed to be negligible and complete combustion ($\eta_c=1.0$) was assumed for simplicity. If necessary, the effect of η_c can be accounted for by a simple correction to ER assuming any unburned fuel is in pseudo-equilibrium with the combustion products and possessing the same state properties.

The calculated values of maximum net engine thrust coefficient,

$$C_{T_{n,\max}}=C_{T_{g,\max}}-C_{D_I}$$

at a given M_0 (4, 5, 6, or 7) were then plotted as a function of fuel-air equivalence ratio ER for each combination of A_i/A_1, A_4/A_2, and A_5/A_i. Only $C_{T_{n,\max}}$ was plotted since the intent of this optimization study is to maximize engine thrust. These curves, however, have not been included in this article for brevity and because they are directed at developing the baseline engine design, not assessing its sensitivity to assumptions. The reader is referred to Ref. 19 for the curves and the attendant discussion leading to the following conclusions: 1) For $M_0=4$, the maximum values of $C_{t_{n,\max}}$ occur when $A_i/A_1\simeq 12$, $A_4/A_2\simeq 5$, and $A_5/A_i=2$-3; 2) For $M_0=5$, the maximum values of $C_{T_{n,\max}}$ occur when $A_i/A_1\simeq 12$, $A_4/A_2\simeq 3$, and $A_5/A_i\simeq 3$; 3) For $M_0=6$, the maximum values of $C_{T_{n,\max}}$ occur when $A_i/A_1\simeq 12$,

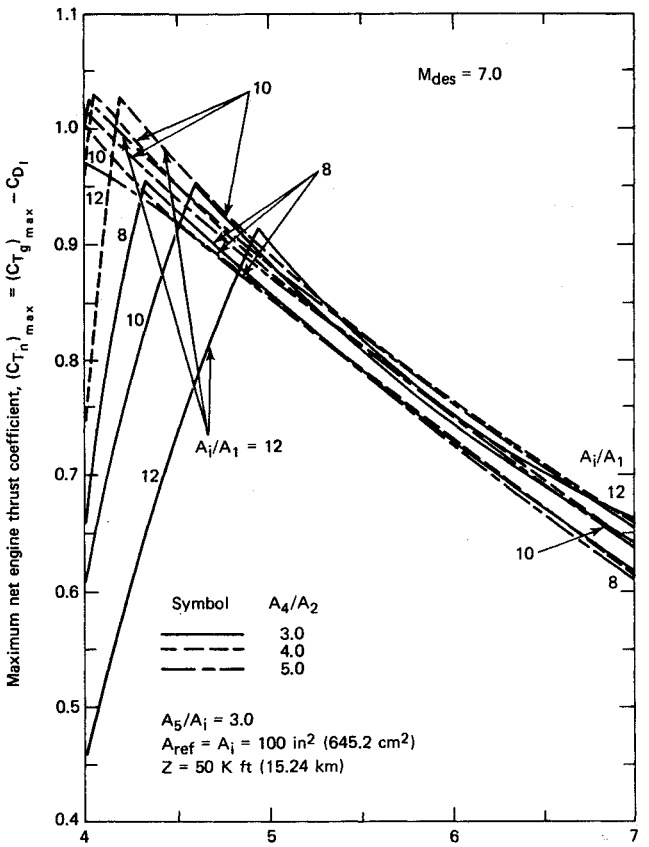

Fig. 5 Maximum net engine-thrust coefficient as a function of flight Mach number for $A_5/A_i = 3.0$, $A_4/A_2 = 3$, 4, and 5, and $A_i/A_1 = 8$, 10, and 12.

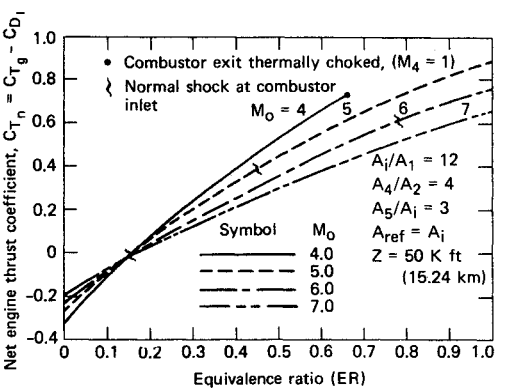

Fig. 6 Net thrust coefficient of optimized engine as a function of fuel-air equivalence ratio and flight Mach number.

$A_4/A_2 \simeq 4$, and $A_5/A_i \simeq 4$; 4) For $M_0 = 7$, the maximum values of $C_{T_{n,max}}$ occur when $A_i/A_1 \simeq 12$, $A_4/A_2 \simeq 3$-5, and $A_5/A_i \simeq 4$; and 5) For $4 < M_0 < 7$, there is only a small gain in $C_{T_{n,max}}$ for $A_i/A_1 \gtrsim 9$-10.

From the results presented above, it is apparent that each M_0 has an optimum value of A_4/A_2 and A_5/A_i. Consequently, in order to choose the optimum values of A_i/A_1, A_4/A_2, and A_5/A_i for this engine, $C_{T_{n,max}}$ was plotted vs M_0 for $A_5/A_i = 2$, 3, and 4; $A_4/A_2 = 3$, 4, and 5; and $A_i/A_1 = 8$, 10, and 12. A representative example of these plots is shown in Fig. 5 where $C_{T_{n,max}}$ is plotted as a function of M_0, A_i/A_1, and A_4/A_2 for $A_5/A_i = 3$. Although several different criteria could be used to select A_i/A_1, A_4/A_2, and A_5/A_i, the one chosen herein is simply the highest average value of $C_{T_{n,max}}$ for $M_0 = 4$-7 flight which can be found by integrating the area under the curves. With this done, the optimum fixed-geometry, two-dimensional scramjet engine meeting the constraints and design criteria of this study has $A_i/A_1 = 12$,

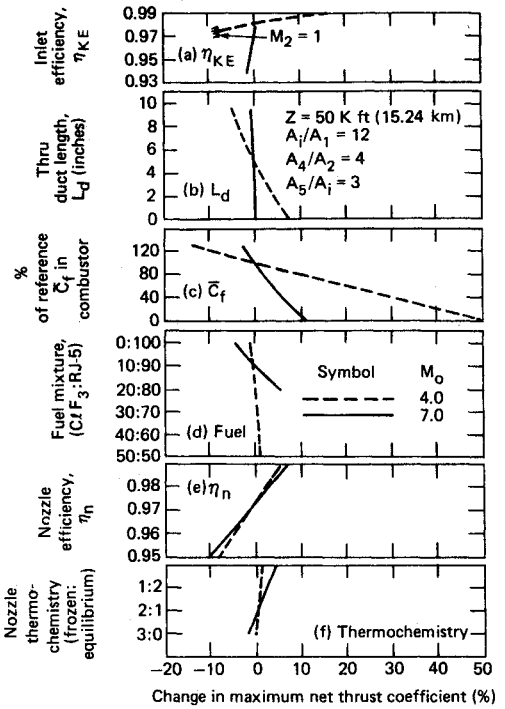

Fig. 7 Sensitivity of optimized engine maximum net thrust coefficient to changes in η_{KE}, L_d, $\bar{C}_f$, fuel composition, η_n, and nozzle thermochemistry for $M_0 = 4$ and 7.

$A_4/A_2 = 4$, and $A_5/A_i = 3$. The corresponding optimum nozzle length L_n is 45 in. (114.3 cm) (Ref. 17).

To complete this engine optimization, C_{T_n} is plotted as a function of ER for $M_0 = 4$-7 in Fig. 6 assuming $\eta_c = 1.0$. Note that ER_{max} at $M_0 = 4$ is 0.66, but is 1.00 for $M_0 \geq 5$. Here, stoichiometry f_s is 0.1008 at $M_0 = 4$, 0.0874 at $M_0 = 5$, and 0.0819 at $M_0 = 6$ and 7 because of the different fuel/pilot mixtures required. The ER's at which a normal shock-pressure rise occurs at the combustor entrance are also noted for $M_0 = 4$, 5, and 6. To the left of these points, an oblique shock pressure rise is present and the combustion process is entirely supersonic. To the right, the combustion process begins in a subsonic flow but $M_4 \geq 1$. For the $M_0 = 7$ case, the combustion process is supersonic at all values of ER.

Engine-Performance-Sensitivity Study

With the optimum engine design established, it is now possible to illustrate the effects of changing η_{KE}, L_d, $\bar{C}_f$ (or L_c), fuel type or mixture, η_n, and nozzle thermochemistry from the previously discussed norms on overall engine thrust. For simplicity, only the $M_0 = 4$ and 7 cases have been considered. In this portion of the study, η_{KE} was varied between 0.99 and 0.975 at $M_0 = 4$ and 0.9775 and 0.9375 at $M_0 = 7$. These correspond approximately to $+11/-5\%$ and $+68/-36\%$ changes in the inlet's supersonic total pressure recovery P_{t_1}/P_{t_0} at $M_0 = 4$ and 7, respectively. L_d was varied from 10 in. (25.4 cm) to 0 in. in length. $\bar{C}_f$ was varied from0 to 130% of the value given in Fig. 4. η_n was varied between 0.99 and 0.95, and the nozzle expansion was varied from all equilibrium to all frozen flow. In each case, only one parameter at a time was varied in order to illustrate its effect on engine performance. A_i/A_1, A_4/A_2, A_5/A_i, and L_n were held constant at the optimum values determined in the previous section.

Figure 7 presents the resulting percentage change in $C_{T_{n,max}}$ as a function of each of these variables for $M_0 = 4$ (dashed lines) and 7 (solid lines) flight at 50,000 ft (15.24 km) altitude assuming $\eta_c = 1.0$. Here, the percent change in $C_{T_{n,max}}$ is defined at

$$[C_{T_{n,max}} - C_{T_{n,max,ref}}]/C_{T_{n,max,ref}}$$

where the reference value corresponds to $C_{Tn,max}$ of the optimized engine (Fig. 6). From Fig. 7, it is apparent that each of the variations affect engine performance, some more than others. The most significant changes in predicted engine performance occur when the values used for combustor wall shear $\bar{C}_f$ (Fig. 7c) are increased or decreased from the norms presented in Fig. 4 for $M_0 = 4$. In this case, if the assumption is made that the combustor wall skin friction losses are trivial, i.e., $\bar{C}_f = 0$ which is nearly the case in a subsonic combustion ramjet, then the predicted value of engine thrust would be ~49% higher than that for the realistic assumptions used herein. Part of this increase is due to the fact that lowering $\bar{C}_f$ permits more heat to be added at $M_0 = 4$ before the $M_4 = 1$ condition is reached. In fact, when $\bar{C}_f = 0$, $ER_{max} = 1$ as contrasted to the value of 0.66 for the realistically optimized engine (Fig. 6). At $M_0 = 7$, the effects of changes in $\bar{C}_f$ are mitigated somewhat, but are still significant. Assuming $\bar{C}_f = 0$ at $M_0 = 7$ will result in an overprediction of $C_{Tn,max}$ by about 11% even though $ER_{max} = 1$ in all cases.

If η_{KE} is increased from 0.98 to 0.99 at $M_0 = 4$, then $C_{Tn,max}$ will increase by ~17%. These large increases in $C_{Tn,max}$ corresponding to moderate increases in η_{KE} occur because more heat addition is permitted before the $M_4 = 1$ condition is reached, i.e., ER_{max} increases as η_{KE} (or M_2) increases when $M_0 = 4$. Alternatively, lowering η_{KE} at $M_0 = 4$ from 0.98 to 0.975, which is the value of η_{KE} that results in choking at the air duct's exit ($M_2 = 1$), reduces $C_{Tn,max}$ by 7.5%. This condition suggests that $A_i/A_1 = 12$ is too large in the initial optimized design of the previous section because a small change in η_{KE} would give $M_2 = 1$. Consequently, one should consider using a lower value of A_i/A_1, e.g., $10 \le A_i/A_1 < 12$, in subsequent optimization procedures for this engine, even though the integrated average $C_{Tn,max}$ is somewhat lower. Note also that the total pressure loss across the bow shock at zero angle of attack at $M_0 = 4$ for the 15-deg wedge inlet considered in this study corresponds to $\eta_{KE} = 0.982$, and increasing η_{KE} to this value only increases $C_{Tn,max}$ by ~2%. Lower wedge angles would produce less total pressure loss, but the subsequent compression process to the large contraction ratios considered herein would have a correspondingly higher pressure loss; so $\eta_{KE} = 0.982$ is a reasonable upper limit. At $M_0 = 7$, the effect of varying η_{KE} on $C_{Tn,max}$ is small. Increasing P_{t_1}/P_{t_0} by ~68% only increased $C_{Tn,max}$ by ~1%. Here the gain in inlet total-pressure recovery is nearly offset by the higher combustor total-pressure losses due to the higher average combustor Mach number. $ER_{max} = 1$ in all cases at $M_0 = 7$.

Variations in nozzle efficiency η_n at $M_0 = 4$ and 7 (Fig. 7e), air duct length L_d at $M_0 = 4$ (Fig. 7b) and fuel mixture at $M_0 = 4$ and 7 (Fig. 7d) have lesser, but still significant, effect on $C_{Tn,max}$. Increasing η_n from the established norm of 0.975 to 0.985 increases $C_{Tn,max}$ by 4 and 6% at $M_0 = 4$ and 7, respectively. If no air duct is included in the engine design to isolate the combustor-shock/boundary-layer interaction region from the inlet, $C_{Tn,max}$ would be increased by 8% at $M_0 = 4$ but by less than 1% at $M_0 = 7$ if there were no other effects other than a reduction in the wall shear losses. In reality the combustor/inlet interaction would decrease A_0/A_i, increase C_{D_I} and significantly reduce $C_{Tn,max}$.

If by some method the ignition and combustion limitations of RJ-5 could be overcome, then $C1F_3$ would not have to be used, thereby greatly simplifying the engine design. This change would also change $C_{Tn,max}$ and the thrust efficiency. Varying the fuel mixture from the 10% $C1F_3$/90% RJ-5 required at $M_0 = 7$ (Table 1, Refs. 4 and 5) to 100% RJ-5 actually decreases $C_{Tn,max}$ by 4% even though ΔH_f for 100% RJ-5 is 5% higher than for the 10%/90% mixtures. The reason for this is that the 10%/90% mixture requires a 12.5% higher fuel flow rate $\dot{w}_f$ at ER = 1. Thus, the net heat input per second ($\Delta H_f \times \dot{w}_f$) of the 10%/90% mixture is 7% higher than for pure RJ-5. On the other hand, the thrust efficiency, i.e., thrust per pound of fuel of pure RJ-5, would be 7% higher than the 10% $C1F_3$/90% RJ-5 mixture. Similar arguments hold for $M_0 = 4$ case. Here, however, the thrust efficiency of the 100% RJ-5 case is 33% better than the 25% $C1F_3$/75% RJ-5 reference case even though the reference case has a 1% higher $C_{Tn,max}$.

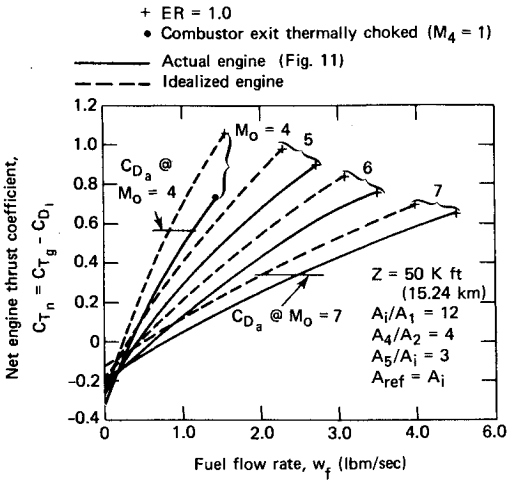

Fig. 8 Comparison of idealized and actual optimum net engine thrust coefficient as a function of fuel flow rate and flight Mach number. + ER = 1.0; combustor exit thermally choked ($M_4 = 1$); solid line, actual engine (Fig. 11); dotted line, idealized engine.

Varying the thermochemistry of the expansion process in the exit nozzle (Fig. 7f) has the smallest effect on $C_{Tn,max}$ of the parameters studied. If it is assumed that the flow is entirely in equilibrium, then the predicted $C_{Tn,max}$ will increase by 1 and 4% at $M_0 = 4$ and 7, respectively. Conversely, assuming completely frozen nozzle flow reduces $C_{Tn,max}$ by 0.5 and 2% at $M_0 = 4$ and 7, respectively.

Comparison of Actual and Ideal Engine and Vehicle Performance

Having illustrated the effects that individual variations in the substantiated norms have on overall engine performance, an additional exemplary case, comparing the predicted engine performance of the optimum engine previously discussed (Fig. 6) with one in which all of the more idealistic assumptions are made, will be presented. For this ideal engine, it is assumed that $L_d = 0$, $\bar{C}_f = 0$, the fuel is 100% RJ-5, $\eta_n = 0.985$, and equilibrium thermochemistry is everywhere present throughout the engine. η_{KE} was not changed from the original values because of its small effect on engine performance at $M_0 = 7$ and the upper and lower bounds for a 15-deg wedge previously discussed. A_i/A_1, A_4/A_2, A_5/A_i, and L_n are the same for both engines. This comparison is intended to demonstratively show the large errors in predicted performance that can result if nonrealistic design criteria are used.

Figure 8 presents the resulting curves of C_{T_n} as a function of $\dot{w}_f$ for $\eta_c = 1.0$ for $M_0 = 4$-7 flight at $Z = 50{,}000$ ft (15.24 km), with the solid lines corresponding to the actual engine (Fig. 6) and the dashed lines corresponding to the idealized engine. Here, $\dot{w}_f$ is used as the abscissa since f_s is different in both cases at the same M_0 (see Table 1). In all cases but the $M_0 = 4$ actual engine case, the curves are terminated on the right at ER = 1.0. Also included are the estimated vehicle axial drag coefficients C_{D_a} at $M_0 = 4$ ($C_{D_a} = 0.566$) and 7 ($C_{D_a} = 0.345$) based on A_i. These were computed assuming a 16 in. (40.6 cm) diam by 150-in. (381-cm) long cylindrical body with a 3/4 power nose and three tail control surfaces and include the engine's external friction drag, but no base drag.

From Fig. 8, it is apparent that the predicted values of C_{T_n} for the idealized engine are substantially higher than those for the realistic engine at a given $\dot{w}_f$ and M_0, with these differences being greater at $M_0 = 4$. At $M_0 = 4$, $C_{Tn,max}$ of the

ideal engine is ~45% higher than that for the realistic engine while at $M_0 = 5$, 6, and 7, these differences are ~9, 12, and 7%, respectively. However, the values of C_{T_n} of the realistic engine at the $\dot{w}_f$ corresponding to $C_{T_{n,\max}}$ of the ideal engine are 27, 22, and 19% lower for $M_0 = 5$, 6, and 7, respectively. In addition, if a vehicle weight of 1500 lbm (681 kg) is assumed, then the realistic engine will have a maximum of only 0.2 g of horizontal axial acceleration $n_{A_{\max}}$ at $M_0 = 4$ and 1.2 g at $M_0 = 7$. Conversely, the values of $n_{A_{\max}}$ are 194% and 13% higher at $M_0 = 4$ and 7, respectively, for the idealized engine. This inherent characteristic of relatively low-accelerative capability of the aft-entry scramjet generally eliminates it from consideration as a candidate concept for applications requiring high acceleration.

Finally, the idealized engine design would require less fuel than the realistic engine at a given thrust level and M_0. This, in turn, results in an overly optimistic powered range when compared to that of the realistic engine, even when fuel density difference are taken into account. For example, for cruise at $M_0 = 7$, the idealized engine would use 0.0301 ft^3/s (0.852 liters/s) of fuel or ~15% less than the realistic engine. For cruise at $M_0 = 4$, this difference is even large. In this case, the idealized engine would burn 0.0123 ft^3/s (0.348 liters/s) of fuel whereas the realistic engine would use 0.0154 ft^3/s (0.436 liters/s), a difference of 20%.

Concluding Remarks

The basis for establishing norms for determining scramjet engine component geometry, length, efficiency, and chemical kinetics has been presented and discussed. An exemplary engine design based on the optimization procedure of Ref. 1 using these norms has been presented and used to illustrate the sensitivity of overall engine performance to deviations from these norms. The special considerations in engine geometry that are needed to produce a viable scramjet engine, especially when selecting the inlet area contraction ratio and combustor exit-to-inlet area ratio are illustrated. It is shown that the engine preformance is quite sensitive to variations in the assumed values for combustor wall friction losses and to variations in the fuel/pilot mixure at the lower M_0 values and nozzle efficiency at all M_0 values. Variations in inlet kinetic-energy efficiency, air-duct length, and nozzle thermochemistry affect engine performance, but to a lesser degree.

A comparative study of an idealized engine with a realistic engine has also been presented. The results demonstrate that if overly optimistic assumptions are made, then the maximum predicted net engine thrust can be overestimated by as much as 45%, the accelerative ability by 194%, and the fuel efficiency by 20%. Consequently, it is of paramount importance that the correct component norms for the determining geometry, length, efficiency, and thermochemistry be used when designing the engine and predicting its performance.

Acknowledgments

This work was supported by the U.S. Navy under Naval Sea Systems Command Contract N00024-78-C-5384. The authors are indebted to J. Murrin (NAVSEA-62R2) for his sponsorship and support of this effort.

References

[1] Waltrup, P.J., Billig, F.S., and Stockbridge, R.D., "A Procedure for Optimizing the Design of Scramjet Engines," AIAA Preprint No. 78-1110 presented at the AIAA/SAE 14th Joint Propulsion Conference, Las Vegas, Nev., July 25-27, 1978, also *Journal of Spacecraft and Rockets,* Vol. 16, May-June 1979, pp. 163-172.

[2] Waltrup, P.J., Anderson, G.Y., and Stull, F.D., "Supersonic Combustion Ramjet (Scramjet) Engine Performance Development in the United States," *3rd International Symposium on Air Breathing Engines,* Munich, Germany, March 1976, JHU/APL Preprint 76-042.

[3] Hunt, J.L., Lawing, P.L., Marcus, D.C., and Cubbage, J.M., "Conceptual Study of Hypersonic Missiles," AIAA 78-6, presented at the AIAA 16th Aerospace Science Meeting, Huntsvill, Ala., Jan. 16-18, 1978.

[4] Heins, Jr. A.E., Reed, G.J., and Woodgrift, K.W., "Hydrocarbon Scramjet Feasibility Program, Part II. Experimental Investigation of a Hydrocarbon Fueled Scramjet Combustor," AFAPL-TR-70-74, Jan. 1971.

[5] Heins, Jr. A.E., Reed, G.J., and Woodgrift, K.W., "Hydrocarbon Scramjet Feasibility Program, Part III. Free Jet Engine Design and Performance," AFAPL-TR-70-74, Jan. 1971.

[6] Billig, F.S., Dugger, G.L., and Waltrup, P.J., "Inlet-Combustor Interface Problems in Scramjet Engines," *1st International Symposium on Air Breathing Engines,* Marseille, France, June 1972.

[7] Waltrup, P.J. and Billig, F.S., "The Structure of Shock Waves in Cylindrical Ducts," *AIAA Journal,* Vol. 11, Oct. 1973, pp. 1404-1408.

[8] Waltrup, P.J. and Billig, F.S., "Prediction of Precombustion Wall Pressure Distributions in Scramjet Engines," *Journal of Spacecraft and Rockets,* Vol. 10, Sept. 1973, pp. 620-622.

[9] Waltrup, P.J. and Cameron, J.M., "Wall Shear and Boundary Layer Measurements in Shock Separated Flow," *AIAA Journal,* Vol. 12, June 1974, pp. 878-880.

[10] Perini, L.L., "Curve Fits of JANNAF Thermochemical Data," APL/JHU ANSP-M-5, Sept. 1972.

[11] Cruise, D.R., "Notes on the Rapid Computation of Chemical Equilibria," *Journal of Physical Chemistry,* Vol. 68, 1964, p. 3797.

[12] Billig, F.S., "Design of Supersonic Combustors Based on Pressure-Area Fields," *11th Symposium (International) on Combustion,* The Combustion Institute, Pittsburgh, Pa., 1967, pp. 755-759.

[13] Billig, F.S. and Dugger, G.L., "The Interaction of Shock Waves and Heat Addition in the Design of Supersonic Combustors," *12th Symposium (International) on Combustion,* The Combustion Institute, Pittsburgh, Pa., 1968, pp. 1125-1134.

[14] Billig, F.S. and Grenleski, S.E., "Experiments and Analysis of Heat Transfer in Supersonic Combustion Processes," *Fourth International Heat Transfer Conference,* Paris, Versailles, Aug. 1970, Vol. 3, Elsevier Publishing Company, Amsterdam, 1970.

[15] Eckert, E.R.E., "Engineering Relations for Friction and Heat Transfer to Surfaces in High Velocity Flows," *Journal of Aeronautical Science,* Vol. 22, 1955, pp. 585-587.

[16] Schetz, J.A., Billig, F.S., and Favin, S., "Analysis of Mixing and Combustion in a Scramjet Combustor with a Coaxial Fuel Jet," presented at the AIAA/SAE/ASME Joint Propulsion Conference, AIAA 80-1256, Hartford, Conn., June 30-July 2, 1980.

[17] Agosta, V. and Hammer, S., "Scramjet Nozzle Analysis," PSI Rept. 70-1, Propulsion Sciences, Inc., Melville, N.Y., Feb. 1970.

[18] Fehlner, L.F. and Nice, E.V., "Tabulation of Standard Atmospheres at 100-Foot Intervals of Altitude," APL/JHU TG 313-1, Aug. 1968.

[19] Waltrup, P.J., Billig, F.S., and Evans, M.C., "Critical Considerations in the Design of Supersonic Combustion Ramjet (Scramjet) Engines," AIAA Paper 80-1284, presented at AIAA/SAE/ASME 16th Joint Propulsion Conference, Hartford, Conn., June 30-July 2, 1980.